

# Journal of Materials Chemistry A

Accepted Manuscript



This is an *Accepted Manuscript*, which has been through the Royal Society of Chemistry peer review process and has been accepted for publication.

*Accepted Manuscripts* are published online shortly after acceptance, before technical editing, formatting and proof reading. Using this free service, authors can make their results available to the community, in citable form, before we publish the edited article. We will replace this *Accepted Manuscript* with the edited and formatted *Advance Article* as soon as it is available.

You can find more information about *Accepted Manuscripts* in the [Information for Authors](#).

Please note that technical editing may introduce minor changes to the text and/or graphics, which may alter content. The journal's standard [Terms & Conditions](#) and the [Ethical guidelines](#) still apply. In no event shall the Royal Society of Chemistry be held responsible for any errors or omissions in this *Accepted Manuscript* or any consequences arising from the use of any information it contains.



Journal Name

COMMUNICATION

## A one-step electrodeposition of homogeneous and vertically aligned nanotubes with parahydrophobic properties (high water adhesion)

Received 00th January 20xx,  
Accepted 00th January 20xx

DOI: 10.1039/x0xx00000x

Thierry Darmanin and Frédéric Guittard

www.rsc.org/

Here, we report for the first time parahydrophobic (high water adhesion) vertically aligned nanotubes by a one-step electropolymerization of naphtho[2,3-b]thieno[3,4-e][1,4]dioxine (NaphDOT) without surfactant and hard template. The formation of nanotubes is probably due to the stabilization by the polymer of gas bubbles produced *in-situ* during electropolymerization process. The nanotubes are obtained by cyclic voltammetry or at constant potential, but their formation is highly dependent on the deposition method. By cyclic voltammetry, the size of the nanotubes is extremely large ( $\varnothing \approx 300$  nm) and independent of the number of deposition scans, while only the density of nanotubes increases. At constant potential, all the seeds for the nanotube formation are created in the first moments, while the size of the nanotube increases with the deposition charge. Here,  $\theta_w$  up to  $135^\circ$  are obtained even if the polymer is intrinsically highly hydrophilic (Young angle  $\theta^y = 63.6^\circ$ ). Moreover, water droplets put on these substrates remain stuck even after an inclination of  $90^\circ$  revealing extremely high adhesion. Such materials could be used in water transportation and harvesting, energy systems and biosensing.

### Introduction

In nature, many plants and insects possess special wetting properties.<sup>1</sup> Amongst them, species having superhydrophobic properties, characterized by high water contact angles ( $\theta_w$ ) and low water adhesion or hysteresis ( $H$ ), are completely resistant to water wetting during rainfalls or have the ability to walk on water surfaces, for example.<sup>2-4</sup> By contrast, other species having parahydrophobic properties,<sup>5</sup> characterized by high water contact angles ( $\theta_w$ ) but also high water adhesion are

able to capture water droplets even in hot environments. This is the case of rose petals, gecko feet and peach skin.<sup>6-9</sup> Materials with high water adhesion are in high demand for different applications, especially for water harvesting and transportation.<sup>10-12</sup> Usually, superhydrophobic properties with high robustness can be reached combining surface structures often at a micro/nanoscale with low surface energy materials.<sup>13,14</sup> For parahydrophobic properties, the water adhesion can be increased by modifying the shape of the surface structures and/or using materials of higher surface energy.<sup>15-21</sup> For example, Li et al. reported the formation of parahydrophobic silver nanostructures by electroless galvanic deposition and without any surface *post*-functionalization.<sup>18</sup> In their work, parahydrophobic properties were obtained after surface oxidation by storage showing the importance of the surface energy. Moreover, the parahydrophobic properties can also be controlled with the shape of the nanostructures as a function of the deposition conditions.

Both surface structures and surface energy can be easily controlled using conducting materials. There are many strategies employed to obtain nanostructured conducting polymers with various shapes.<sup>22,23</sup> These nanostructured materials can be produced in solution by self-assembly but in order to reduce the number of steps, it is preferable to induce the formation of nanostructures directly on substrates. This is possible by different methods including preferential growth, vapor phase polymerization, plasma polymerization and electropolymerization.<sup>22,23</sup> Electropolymerization allows rapid deposition of conducting polymer films with a wide variety of monomers. Amongst all the available polymerizable cores, 3,4-ethylenedioxythiophene (EDOT) and its derivatives are probably the most interesting for both their exceptional polymerization capacity<sup>24</sup> but also the extreme variability of the shape of the surface structures with the electropolymerization conditions<sup>25</sup> and the presence of a substituent.<sup>26-29</sup> For example, nanofibers, spherical particles, nanosheets, flower-like structures and cauliflower-like structures have all been reported. While fluorocarbon and

Univ. Nice Sophia Antipolis, CNRS, LPMC, UMR 7336, Parc Valrose, 06100 Nice, France

† Footnotes relating to the title and/or authors should appear here.

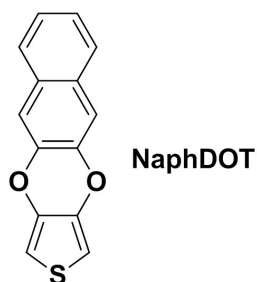
Electronic Supplementary Information (ESI) available: [details of any supplementary information available should be included here]. See DOI: 10.1039/x0xx00000x

hydrocarbon chains were often used to reach superhydrophobic properties, parahydrophobicity can be obtained using substituents of higher surface energy. This is possible using branched hydrocarbon chains or aromatic substituents (phenyl, naphthalene, pyrene, etc).<sup>30,31</sup>

Here, we report for the first time the formation of conducting polymer nanotubes with parahydrophobic properties. Conducting nanotubes are excellent candidates for various applications in electronic devices for energy systems and biosensing.<sup>32-34</sup> However, the methods to develop vertically aligned nanotubes on various substrates are often lengthy or need specific or expensive equipment.<sup>35-42</sup> For example, densely packed carbon nanotubes were reported by chemical vapor deposition.<sup>36,37</sup> Superhydrophobic properties were obtained after a post-treatment with PTFE coating. Otherwise, titanium nanotubes can also be created by anodization but highly corrosive fluorinated electrolytes are necessary.<sup>38</sup> Aligned polystyrene nanotubes were also fabricated via solution casting or by electrodeposition/electropolymerization using an anodized aluminum oxide (AAO) membrane as hard template, which was later dissolved in NaOH solution to obtain nanotubes.<sup>16,17,39</sup>

Hence, methods to develop in one-step and very quickly nanotubes on substrates are not numerous. In the literature, we have found only one process related to the works of Prof. Shi and co-authors who formed nanotubes by direct electropolymerization of pyrrole in an aqueous solution of a surfactant ( $\beta$ -naphthalenesulfonic acid, (+)- and (-)-camphorsulfonic acids or poly(styrene sulfonic acid).<sup>43-46</sup> The aim of the surfactant was to stabilize gas bubbles produced *in-situ*.

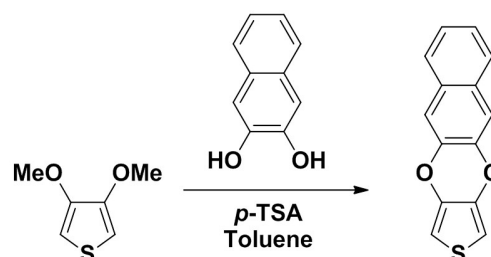
Here, first we show for the first time that it is possible to obtain nanotubes in organic solvents, which is extremely important because most of the monomers are not soluble in water. More precisely, the nanotubes are obtained by a one-step electropolymerization of an EDOT derivative grafted with a naphthalene moiety. The very rigid EDOT derivative named naphtho[2,3-*b*]thieno[3,4-*e*][1,4]dioxine or NaphDOT is represented in **Scheme 1**. We also explore for the first time the possibility to obtain parahydrophobic properties with this process. The influence of the electrodeposition conditions and monomer nature on the formation of nanotubes and their parahydrophobic properties is discussed as well as the mechanism of the nanotube formation.



**Scheme 1** Monomer used in this work to obtain nanotubes.

## Materials and methods

The monomer NaphDOT was synthesized following a procedure reported in the literature by transesterification between 3,4-dimethoxythiophene and 2,3-naphthalenediol (Scheme 2).<sup>47</sup> More precisely, 2.5 g of 3,4-dimethoxythiophene (17.4 mmol, 1 eq.), 10 g of 2,3-naphthalenediol (62.4 mmol, 3.6 eq.), 0.5 g of *p*-toluenesulfonic acid monohydrate (2.6 mmol, 0.15 eq.) was added to 120 mL of toluene. The mixture was stirred and heated at 100°C for 2 days. Then, 80 mL of the solvent was removed by rotavapor and the product was purified by column chromatography (silica gel; eluent: dichloromethane/cyclohexane 1:1). The spectra of the monomer characterization are given in ESI.



**Scheme 2** Synthetic way to the monomer.

**NaphDOT:** naphtho[2,3-*b*]thieno[3,4-*e*][1,4]dioxine. Yield: 10%; White solid; m.p.: 205.8°C;  $\delta_{\text{H}}$ (200 MHz,  $\text{CDCl}_3$ , ppm): 7.67 (m, 2H), 7.36 (m, 4H), 6.52 (s, 2H);  $\delta_{\text{C}}$ (200 MHz,  $\text{CDCl}_3$ , ppm): 140.62, 138.74, 130.47, 126.79, 125.32, 112.57, 101.05; FTIR (KBr):  $\nu_{\text{max}}$ / $\text{cm}^{-1}$  3107, 2955, 2925, 2850, 1513, 1505, 1476, 1441, 1278, 873, 762  $\text{cm}^{-1}$ ; MS (70 eV)  $m/z$  (%): 240 (100) [ $\text{M}^+$ ].

The conducting polymer films were electrodeposited on gold plates used as working electrodes. A carbon rod and a saturated calomel electrode (SCE) were used as a counter-electrode and reference electrode, respectively. The electrodes were inserted in 10 mL anhydrous dichloromethane containing 0.1 of tetrabutylammonium perchlorate ( $\text{Bu}_4\text{NClO}_4$ ) and 0.01 M of NaphDOT. In order to perform the electrodeposition, the electrodes were connected to an Autolab potentiostat of Metrohm. Two different deposition methods were used in order to study its influence on the polymer growth:

- cyclic voltammetry from -1.00 V to 1.80 V vs SCE at a scan rate of 20  $\text{mV s}^{-1}$  and using different deposition scans (1, 3, 5);
- imposed potential or chronoamperometry at 1.80 V vs SCE and using different deposition charges (12.5, 25, 50, 100, 200, 400  $\text{mC cm}^{-2}$ ).

After the depositions, the substrates were washed in three different solutions of dichloromethane and slowly dried.

The surface properties were characterized by scanning electron microscopy (SEM), optical profilometry and goniometry. The SEM images were taken using a 6700F

microscope of JEOL. An ultra-thin surface metallization was performed before each measurement to improve the image quality. The arithmetic ( $R_a$ ) and quadratic ( $R_q$ ) surface roughness were obtained using a Wyko NT 1100 optical microscope of Bruker. The measurements were performed with High Mag Phase Shift Interference (PSI) working mode, the field of view (FOV) 0.5X and the objective 50X. The surface wettability was investigated using a DSA30 goniometer of Krüss. The water apparent contact angles ( $\theta$ ) were determined by taking the angle at the triple point of 2  $\mu\text{L}$  water droplets placed on the substrates. Otherwise, the tilted-drop method was used to determine the hysteresis ( $H$ ) and sliding angle ( $\alpha$ ). Here, a 6  $\mu\text{L}$  water droplet was put on the substrate and it was inclined until the droplet moved. If the droplet moved,  $H$  was taken just before it moved. If the droplet did not move even for  $\alpha = 90^\circ$ , the substrate was called sticky.

## Results and Discussion

First, the monomer was electropolymerized by cyclic voltammetry in anhydrous dichloromethane containing 0.1 M of  $\text{Bu}_4\text{NClO}_4$  and at a scan rate of  $20 \text{ mV s}^{-1}$ . In order to study the influence of the polymer growth on the surface properties, the polymerization was stopped after different deposition scans (1, 3 and 5). The cyclic voltammogram after 5 deposition scans is given in Figure 1. This voltammogram shows that the polymer thickness does not significantly increase as the number of deposition scans which may be explained by a decrease in the polymer conductivity. Moreover, a peak at about  $-0.3 \text{ V}$  vs SCE, which should correspond to the formation of  $\text{H}_2$  from  $\text{H}^+$ , is present during each back scan. The presence of this peak is extremely important in the formation of nanotubes.<sup>43-45</sup>

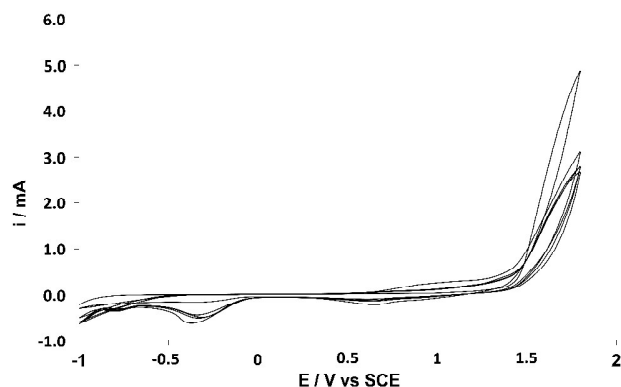


**Fig. 1** Cyclic voltammogram (5 scans) of NaphDOT in 0.1 M  $\text{Bu}_4\text{NClO}_4$ /anhydrous acetonitrile; scan rate:  $20 \text{ mV s}^{-1}$ .

Then, the polymer films were characterized by contact angle measurements, optical profilometry and SEM. Table 1 indicates that  $\theta$  increases as the number deposition scans increases from 1 to 3, reaching a maximum ( $\theta = 135.0^\circ$ ) for 3 deposition scans.  $\theta$  remains the same for 3 or 5 deposition scans. Experiments with the tilted-drop method showed the extremely high water adhesion of these substrates. A water

droplet put on these substrates remained completely stuck even after an inclination of  $90^\circ$ , as shown in Figure 2.

**Table 1** Roughness and apparent contact angles as a function of the deposition method.

Deposition characteristics	$R_a$ [nm]	$R_q$ [nm]	$\theta$ [deg]
CV 1 scan	40	58	113.7
CV 3 scan	550	750	135.0
CV 5 scan	500	630	134.4
CP $12.5 \text{ mC cm}^{-2}$	9	16	130.0
CP $25 \text{ mC cm}^{-2}$	19	50	110.4
CP $50 \text{ mC cm}^{-2}$	20	40	100.0
CP $100 \text{ mC cm}^{-2}$	350	480	79.3
CP $200 \text{ mC cm}^{-2}$	410	610	75.2
CP $400 \text{ mC cm}^{-2}$	750	1300	77.7



**Fig. 2** Picture of a water droplet put on PolyNaphDOT, obtained by cyclic voltammetry (3 scans), and after a surface inclination of  $90^\circ$ .

Moreover, for 3 deposition scans the surface roughness ( $R_a = 550 \text{ nm}$ ) is also very important. Surprisingly, the SEM images revealed the presence of vertically aligned nanotubes (Figure 3). These nanotubes are large ( $\varnothing \approx 300 \text{ nm}$ ) and their height ( $h$ ) is slightly higher than  $1 \mu\text{m}$ . Their dimensions are quite similar after each deposition scan, but the number of nanotubes increases until reaching a maximum after 3 deposition scans. After 3 depositions, the nanotubes begin to be inclined.

In order to determine the effect of the nanotubes on the surface hydrophobicity, it is first necessary to determine the apparent contact angles of the same polymer but smooth (without any structures). The apparent contact angles of smooth substrates are called Young angles ( $\theta^y$ ) are dependent on the solid-vapor ( $\gamma_{sv}$ ), solid-liquid ( $\gamma_{sl}$ ) and liquid-vapor ( $\gamma_{lv}$ ) surface tensions following the Young equation:  $\cos \theta^y = (\gamma_{sv} - \gamma_{sl})/\gamma_{lv}$ . Here, smooth PolyNaphDOT films were produced using a two-step electrodeposition process: a first step at constant potential ( $E = 1.80 \text{ V}$ ) and using an extremely short deposition charges ( $Q_s = 1 \text{ mC cm}^{-2}$ ) in order to cover all the substrate while avoiding the surface structure formation; a second reduction step by cyclic voltammetry from  $1.5 \text{ V}$  to  $-1.0 \text{ V}$  in order to reduce the polymer.

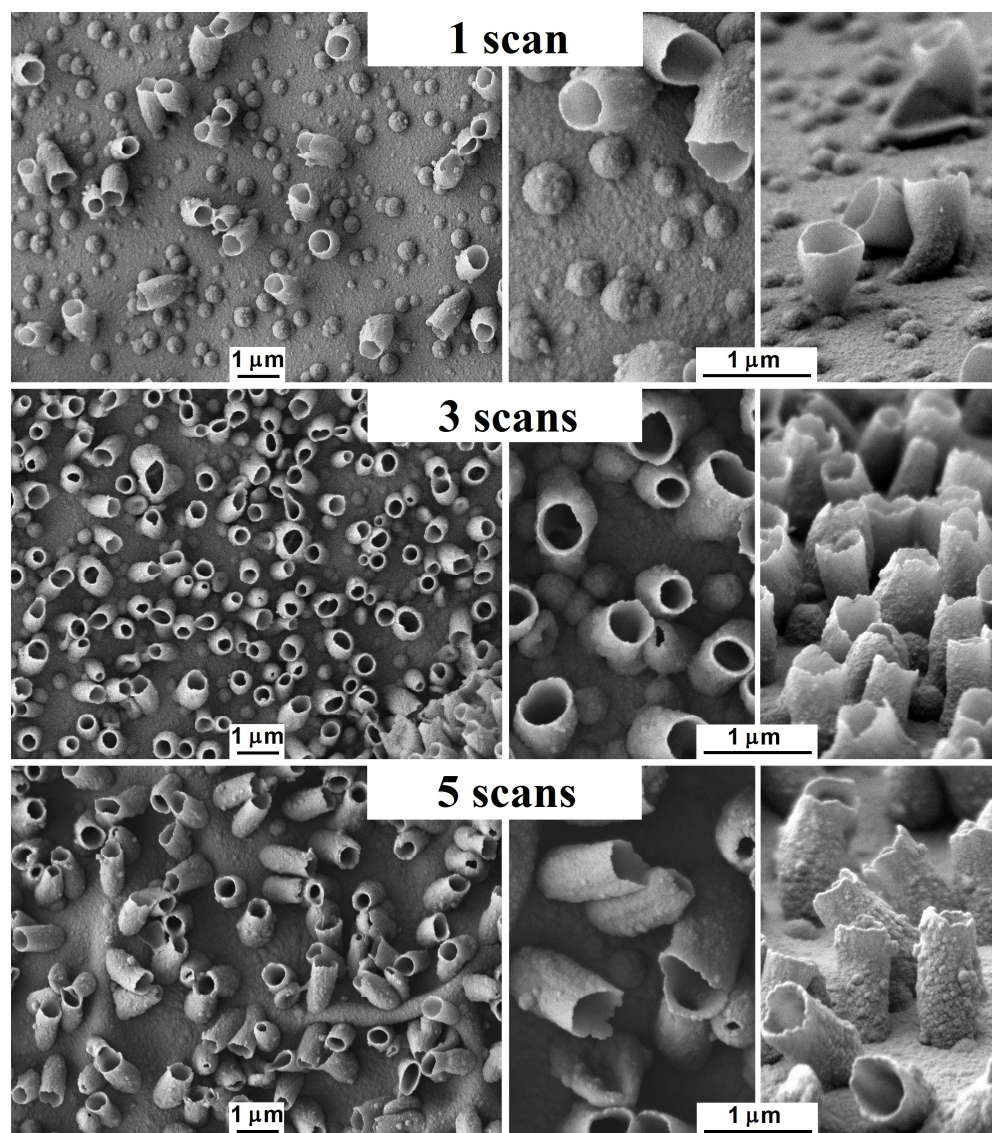


**Fig. 3** On the left, SEM images of PolyNaphDOT at the magnification of 10000x without substrate inclination. On the right, SEM images of PolyNaphDOT at the magnification of 25000x without substrate inclination and with a substrate inclination of 60°. Here, the substrates were obtained by cyclic voltammetry and as a function of the number of deposition scans.

The mean ( $R_a$ ) and quadratic ( $R_q$ ) roughness of these smooth surfaces are 7 nm and 12 nm, respectively. On these smooth substrates,  $\theta^Y$  was found to be 63.6° indicating a high hydrophilic behavior ( $\theta^Y \ll 90^\circ$ ). Because polyNaphDOT is a highly hydrophilic polymer, the parahydrophobic properties cannot be explained with the Wenzel equation  $\cos \theta = r \cos \theta^Y$ , where  $r$  is a roughness parameter.<sup>48</sup> Indeed,  $r$  can increase the surface hydrophobicity only if  $\theta^Y > 90^\circ$ , otherwise it increases the surface hydrophilicity. Only the Cassie-Baxter equation can explain these results, which indicates the presence of air trapped between the water droplet and the substrate. The Cassie-Baxter equation is  $\cos \theta = r_f \cos \theta^Y + f - 1$ , where  $r_f$  is the roughness ratio of the substrate wetted by the liquid,  $f$  is the solid fraction and  $(1 - f)$  is the air fraction.<sup>49</sup>

The Cassie-Baxter equation can describe superhydrophobic properties with very low adhesion if the air fraction is extremely significant but also to parahydrophobic properties if the air fraction is much less important. Moreover, parahydrophobic states are metastable states between the Wenzel and the Cassie-Baxter states and the applying of a high pressure induces the transition to the Wenzel state, here superhydrophilic properties because  $\theta^Y < 90^\circ$ .

The wettability results reported in our work are in agreement with the work of Jiang et al.<sup>16,17</sup> In this work, the authors fabricated aligned polystyrene nanotubes and observed that the substrates with nanotubes were parahydrophobic. One of the main differences between these two works is the intrinsic hydrophobicity of the used materials: the smooth polystyrene

is intrinsically hydrophobic and has a  $\theta$  of  $95^\circ$  while PolyNaphDOT is much more hydrophilic ( $\theta = 63.6^\circ$ ). Moreover, the PolyNaphDOT nanotubes are not densely packed contrary to the polystyrene nanotubes.<sup>16,17</sup> Hence, for the PolyNaphDOT nanotubes the water droplet should penetrate the space between the nanotubes (Wenzel state) which highly increases the water adhesion. However, the PolyNaphDOT nanotubes are parahydrophobic because the water does not penetrate inside the nanotubes (Cassie-Baxter state). The interface is, thus, composite (Figure 4) with the presence of air only inside the nanotubes and as a consequence the parahydrophobic properties are highly dependent on the diameter, height of the nanotubes as well as the distance between them. Moreover, it can be expected that the parahydrophobic properties are also higher if the nanotubes are vertically aligned.

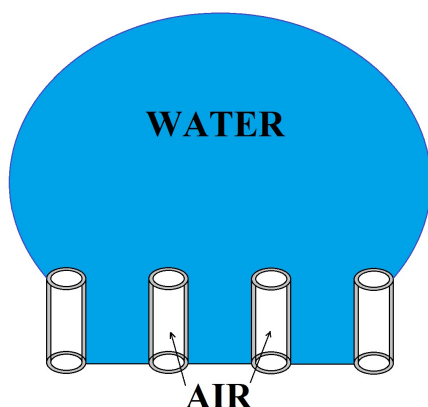


**Fig. 4** Schematic representation of a water droplet deposited on hydrophilic nanotubes.

Hence, large seeds for the formation of nanotubes are created at each deposition scan and the nanotubes are created from these seeds. In order to better explain their formation, we have looked for related publications in the literature and found only one method reported by the research group of Prof. Shi.<sup>43-46</sup> This method consists in the formation of polypyrrole nanotubes or nanocontainers of different sizes by electropolymerization of pyrrole in an aqueous solution of a surfactant ( $\beta$ -naphthalenesulfonic acid, (+)- and (-)-camphorsulfonic acids or poly(styrene sulfonic acid)). The authors demonstrated that the role of the surfactant is to stabilize the  $H_2$  or  $O_2$  bubbles produced *in-situ* either during water electrolysis or the decomposition potential of acidic water, respectively. Hence,  $H_2$  or  $O_2$  bubbles act here as a soft template. Moreover, the authors also showed that in organic media such as acetonitrile, although gas bubbles are produced, they cannot be enwrapped by surfactant and are dispersed in the medium or escape from the solution quickly.<sup>43</sup> Indeed, for example, the electropolymerization released  $H^+$  ions, which can lead to  $H_2$  bubbles. Based on these findings, we can conclude that our work shows that our polymer is able to stabilize these bubbles during electrodeposition without

surfactant. Other experiments showed that the stabilization is possible in dichloromethane and not in acetonitrile. This may be explained by the fact that the oligomers formed in the first instance are more soluble in dichloromethane, which is a probably a key factor to stabilize the bubbles. Other related monomers with only one phenyl ring such as benzo[*b*]thieno[3,4-*e*][1,4]dioxine (PheDOT) or without aromatic ring such as EDOT have also been tested to see if the used monomer is important (c.f. Supporting Information). Nothing special was observed with EDOT but very large and homogeneous holes were observed with PheDOT. Hence, the exceptional capacity of NaphDOT to stabilize bubbles is probably due to the presence of the naphthalene group, as observed by Shi using  $\beta$ -naphthalenesulfonic surfactant.<sup>43-46</sup>

In order to study the influence of the deposition method, PolyNaphDOT was also electrodeposited at constant potential ( $E = 1.80$  V vs SCE) and using different deposition charges ( $Q_s = 12.5, 25, 50, 100, 200$  and  $400$  mC  $cm^{-2}$ ). SEM images are given in Figure 5 and the apparent contact angles and surface roughness are available in Table 1. Completely different results were obtained with this method. This time all the seeds for the formation of the nanotubes are created in the first instance ( $Q_s = 12.5$  mC  $cm^{-2}$ ) and after the size of the nanotubes increases with  $Q_s$ . However, for  $Q_s = 12.5$  mC  $cm^{-2}$  the size of the seeds is extremely low ( $\varnothing \approx 70$  nm,  $h \approx 100$  nm) but the number of seeds is extremely important, which leads to the highest contact angles ( $\theta = 135.0^\circ$ ) even if the roughness is extremely low ( $R_a \approx 10$  nm). Indeed, it is expected that the size of the nanotubes is more important by cyclic voltammetry because a large range of potentials is scanned during this method. Then, the size of the nanotubes increases as  $Q_s$  but  $\theta$  decreases because the porosity percentage in contact to the water droplet decreases. From  $Q_s = 100$  mC  $cm^{-2}$  the size of the nanotubes become very high ( $h$  above  $1 \mu m$ ) and begin to be inclined. Moreover, the opening of the nanotubes also begins to close, which leads to a very large decrease in  $\theta$  ( $\theta < 80^\circ$ ).

## Conclusions

Here, we reported for the time the formation of parahydrophobic vertically aligned nanotubes by electropolymerization of NaphDOT. It seems that the polymer is able to stabilize gas bubbles produced *in-situ* during the electrodeposition, which leads to the nanotube formation. These nanotubes were obtained by cyclic voltammetry or at constant potential but the growth of these nanotubes was highly dependent on the deposition method. By cyclic voltammetry, the size of the nanotubes was extremely large ( $\varnothing \approx 300$  nm) and independent on the number of deposition scans while only the density of nanotubes increased. At constant potential, all the seeds for the nanotube formation were created in the first instances while the size of the nanotubes increased with the deposition charge.

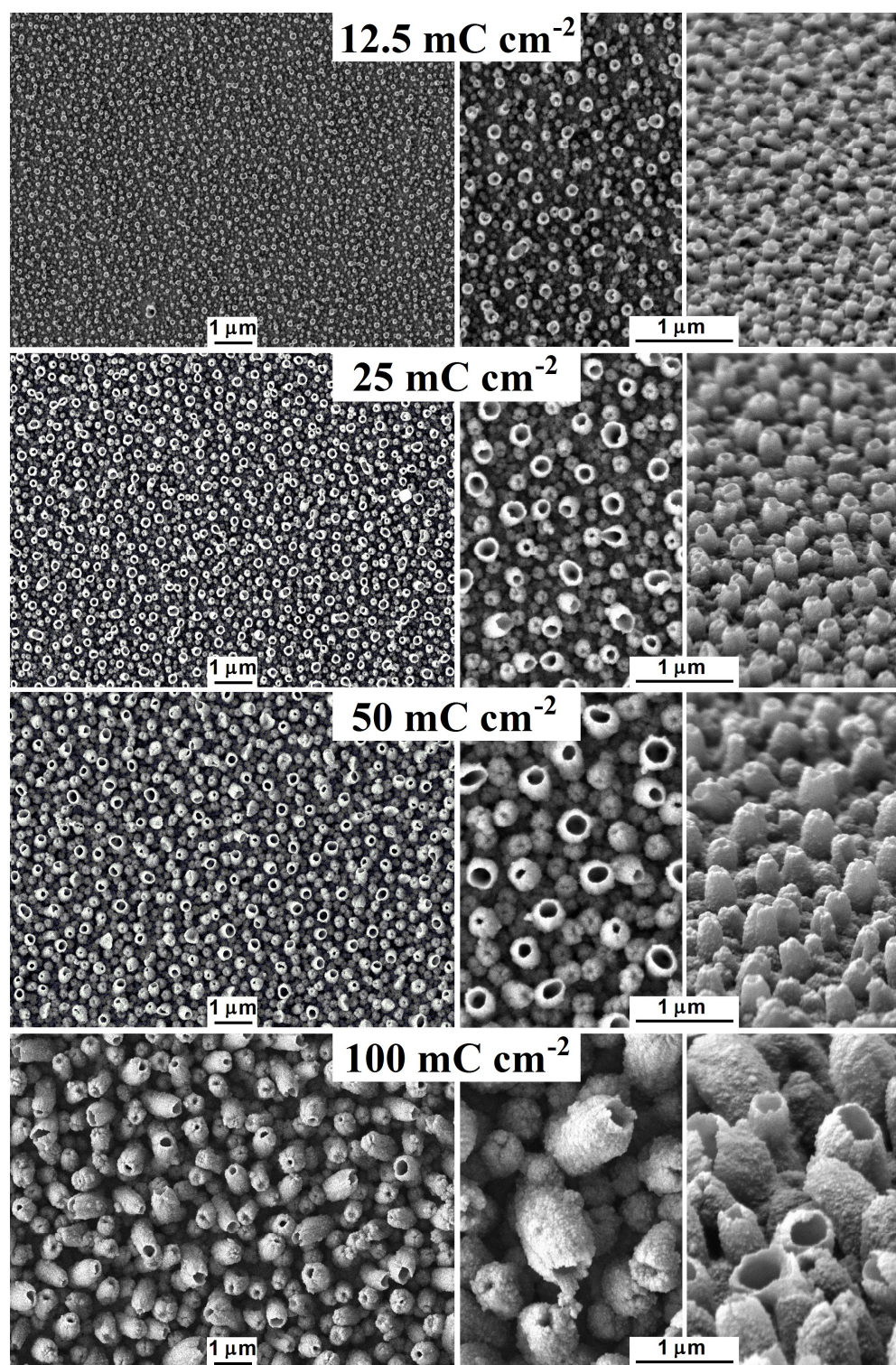


**Fig. 5** On the left, SEM images of PolyNaphDOT at the magnification of 10000x without substrate inclination. On the right, SEM images of PolyNaphDOT at the magnification of 25000x without substrate inclination and with a substrate inclination of 60°. Here, the substrates were obtained at constant potential and as a function of deposition charge.

Here,  $\theta_w$  up to 135° were obtained even if the polymer is intrinsically highly hydrophilic (Young angle  $\theta^y = 63.6^\circ$ ). Moreover, water droplets put on these substrates remained

stuck even after an inclination of 90° revealing extremely high adhesion. This work is the first step in the formation of nanotubes in organic solvent and other monomers will be

studied in the future. Such materials can find applications in water transportation and harvesting, energy systems and biosensing. Indeed, most of these applications need materials with tunable water adhesion.

## Acknowledgment

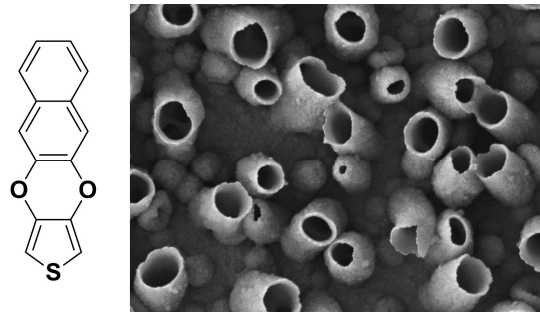
This project was supported by JSPS [KAKENHI, Grant-in-Aid for Young Scientists (A), No. 23685034], RCUK [through EPSRC EP/K020676/1] and ANR-13-G8ME-0003 under the G8 Research Councils Initiative on Multilateral Research Funding - G8-2012.

We thank Jean-Pierre Laugier and François Orange of the Centre Commun de Microscopie Appliquée (CCMA, Univ. Nice Sophia Antipolis) for the realization of the SEM images.

## References

- 1 T. Darmanin and F. Guittard, *F. Mater. Today*, 2015, **18**, 273–285.
- 2 K. Koch, B. Bhushan, W. and Barthlott, *Prog. Mater. Sci.*, 2009, **54**, 137–178.
- 3 J. W. M. Bush, D. L. Hu and M. Prakash, *Adv. Insect Physiol.*, 2007, **34**, 117–192.
- 4 J. Nickerl, R. Helbig, H.-J. Schulz, C. Werner and C. Neinhuis, *Zoomorphology*, 2013, **132**, 83–195.
- 5 A. Marmur, *Soft Matter*, 2012, **8**, 6867–6870.
- 6 K. Liu, J. Du, J. Wu and L. Jiang, *Nanoscale*, 2012, **4**, 768–772.
- 7 L. Feng, Y. Zhang, J. Xi, Y. Zhu, N. Wang, F. Xia and L. Jiang, *Langmuir*, 2008, **24**, 4114–4119.
- 8 J. B. K. Law, A. M. H. Ng, A. Y. He and H. Y. Low, *Langmuir*, 2014, **30**, 325–331.
- 9 X. Lu, H. Cai, Y. Wu, C. Teng, C. Jiang, Y. Zhu and L. Jiang, *Sci. Bull.* 2015, **60**, 453–459.
- 10 X. Hong, X. Gao and L. Jiang, *J. Am. Chem. Soc.*, 2007, **129**, 1478–1479.
- 11 J. Li, Z. Jing, F. Zha, Y. Yang and Q. Wang, Z. Lei, *ACS Appl. Mater. Interfaces*, 2014, **6**, 8868–8877.
- 12 N. J. Shirtcliffe, G. McHale and M. I. Newton, *Langmuir*, 2009, **25**, 14121–14128.
- 13 H. Bellanger, T. Darmanin, E. Taffin de Givenchy and F. Guittard, *Chem. Rev.*, 2014, **114**, 2694–2716.
- 14 A. Sarkar and A.-M. Kietzig, *Soft Matter*, 2015, **11**, 1998–2007.
- 15 H. Zhu, Z. Guo and W. Liu, *Chem. Commun.*, 2014, **50**, 3900–3913.
- 16 M. Jin, X. Feng, L. Feng, T. Sun, J. Zhai, T. Li and L. Jiang, *Adv. Mater.*, 2005, **17**, 1977–1981.
- 17 Z. Cheng, J. Gao and L. Jiang, *Langmuir*, 2010, **26**, 8233–8238.
- 18 Y. Wu, T. Hang, J. Komadina, H. Ling and M. Li, *Nanoscale*, 2014, **6**, 9720–9726.
- 19 B. Bhushan and E. K. Her, *Langmuir*, 2010, **26**, 8207–8217.
- 20 M. Liu, S. Wang, Z. Wei, Y. Song and L. Jiang, *Adv. Mater.*, 2009, **21**, 665–669.
- 21 M. Liu, Y. Zheng, J. Zhai and L. Jiang, *Acc. Chem. Res.*, 2010, **43**, 368–377.
- 22 T. Darmanin and F. Guittard, *Prog. Polym. Sci.*, 2014, **39**, 656–682.
- 23 C. Li, H. Bai and G. Shi, *Chem. Soc. Rev.*, 2009, **38**, 2397–2409.
- 24 R. M. Walczak and J. R. Reynolds, *Adv. Mater.*, 2006, **18**, 1121–1131.
- 25 E. Poverenov, M. Li, A. Bitler and M. Bendikov, *Chem. Mater.*, 2010, **22**, 4019–4025.
- 26 T. Darmanin and F. Guittard, *Adv. Mater. Interfaces*, 2015, **2**, 1500081/1–1500081/7.
- 27 T. Darmanin and F. Guittard, *J. Am. Chem. Soc.*, 2011, **133**, 15627–15634.
- 28 J. El-Maiss, T. Darmanin and F. Guittard, *J. Colloid Interface Sci.*, 2015, **447**, 167–172.
- 29 S.-C. Luo, J. Sekine, B. Zhu, H. Zhao, A. Nakao, H.-h. Yu, *ASC Nano*, 2012, **6**, 3018–3026.
- 30 C. Mortier, T. Darmanin and F. Guittard, *Macromolecules*, 2015, **48**, 5188–5195.
- 31 C. Mortier, T. Darmanin and F. Guittard, *Adv. Eng. Mater.*, 2014, **16**, 1400–1405.
- 32 S. Park, M. Vosguerichian and Z. Bao, *Nanoscale*, 2013, **5**, 1727–1752.
- 33 Q. Zhang, J.-Q. Huang, W.-Z. Qian, Y.-Y. Zhang and F. Wei, *Small*, 2013, **9**, 1237–1265.
- 34 O. S. Kwon, S. J. Park, J. S. Lee, E. Park, T. Kim, H.-W. Park, S. A. You, H. Yoon and J. Jang, *Nano Lett.*, 2012, **12**, 2797–2802.
- 35 Y. Lai, X. Gao, H. Zhuang, J. Huang, C. Lin and L. Jiang, *Adv. Mater.*, 2009, **21**, 3799–3803.
- 36 H. Liu, J. Zhai and L. Jiang, *Soft Matter*, 2006, **2**, 811–821.
- 37 K. K. S. Lau, J. Bico, K. B. K. Teo, M. Chhowalla, G. A. J. Amaratunga, W. I. Milne, G. H. McKinley and K. K. Gleason, *Nano Lett.*, 2003, **3**, 1701–1705.
- 38 Y. Lai, F. Pan, C. Xu, H. Fuchs and L. Chi, *Adv. Mater.*, 2013, **25**, 1682–1686.
- 39 M. Liu, X. Liu, J. Wang, Z. Wei and L. Jiang, *Nano Res.*, 2010, **3**, 670–675.
- 40 Y. Li, W. Cai, G. Duan, B. Cao, F. Sun and Fang Lu, *J. Colloid Interface Sci.*, 2005, **287**, 634–639.
- 41 Y. Li, G. Duan, G. Liu and W. Cai, *Chem. Soc. Rev.*, 2013, **42**, 3614–3627.
- 42 Y. Li, X. J. Huang, S. H. Heo, C. C. Li, Y. K. Choi, W. P. Cai and S. O. Cho, *Langmuir*, 2007, **23**, 2169–2174.
- 43 L. Qu, G. Shi, J. Yuan, G. Han and F. Chen, *J. Electroanal. Chem.*, 2004, **561**, 149–156.
- 44 L. Qu, G. Shi, F. Chen and J. Zhang, *Macromolecules*, 2003, **36**, 1063–1067.
- 45 J. Yuan, L. Qu, D. Zhang and G. Shi, *Chem. Commun.*, 2004, 994–995.
- 46 J. T. Kim, S. K. Seol, J. H. Je, Y. Hwu and G. Margaritondo, *Appl. Phys. Lett.*, 2009, **94**, 034103/1–034103/3.
- 47 E. Poverenov, Y. Sheynin, N. Zamoshchik, A. Patra, G. Leituss, I. F. Perepichka and M. Bendikov, *J. Mater. Chem.*, 2012, **22**, 14645–14655.
- 48 R. N. Wenzel, *Ind. Eng. Chem.*, 1936, **28**, 988–994.
- 49 A. B. D. Cassie and S. Baxter, *Trans. Faraday Soc.*, 1944, **40**, 546–551.

## Graphical Abstract



Nanotubes of various dimension and displaying parahydrophobic properties are obtained by a one-step electropolymerization of naphtho[2,3-b]thieno[3,4-e][1,4]dioxine (NaphDOT) without surfactant or hard template.